Plasmonics (2015) 10:721–727
DOI 10.1007/s11468-014-9858-1

Spectral Splitting Based on Electromagnetically Induced Transparency in Plasmonic Waveguide Resonator System

Zhao Chen · Wenhui Wang · Luna Cui · Li Yu · Gaoyan Duan · Yufang Zhao · Jinghua Xiao

Received: 13 October 2014 / Accepted: 4 December 2014 / Published online: 23 December 2014

Abstract Spectral splitting is numerically investigated based on the electromagnetically induced transparency (EIT) in a nanoscale plasmonic waveguide resonator system, which consists of a square ring resonator coupled with a stub-shaped metal-insulator-metal (MIM) waveguide. Simulation results show that the transparency window can be easily tuned by changing the geometrical parameters of the structure and the material filled in the resonators. By adding another stub or (and) square ring resonator, multi-EIT-like peaks appear in the broadband transmission spectrum, and the physical mechanism is presented. Our compact plasmonic structure may have potential applications for nanoscale optical switching, nanosensor, nanolaser, and slow-light devices in highly integrated optical circuits.

Keywords Surface plasmons · Electromagnetically induced transparency · Coupled resonators · MIM waveguide · Integrated optics devices

Introduction

Surface plasmon polaritons (SPPs) are considered to be the most promising candidate for the realization of highly integrated optical circuits due to their capability to overcome the diffraction limit of light [1]. A mass of devices based on SPPs have been demonstrated experimentally and simulation numerically [2, 3]. For example, Chen et al. experimentally realized an optical response in a dielectric film-coated asymmetric T-shape single slit based on the analog of the electromagnetically induced transparency (EIT) [4]. Lu et al. presented a numerical demonstration of a nanosensor based on Fano resonance in a plasmonic coupled resonator system [5]. Waveguides consisting of an insulator sandwiched between two metals serve as metal-insulator-metal (MIM) waveguides. They have deep subwavelength field confinements and low bend loss and have attracted great interest in highly integrated photonic circuits [6–8]. A large number of devices based on MIM waveguides are designed to achieve various functions, such as filters [9–12], splitters [13, 14], sensors [15], and demultiplexers [16–19]. EIT is a special and counterintuitive phenomenon which occurs in atomic systems due to the quantum destructive interference between the excitation pathways to the atomic upper level [20, 21]. Recently, tremendous attention has been attracted to the studies that EIT-like optical responses can be obtained in classical resonator systems [22], which are easily realized and integrated into the chips. The EIT-like spectral response was also found in many devices, such as the coupled whispering-gallery microresonators [23], grating [24], coupled photonic crystal cavities [25, 26], plasmonic resonator antennas [27], and coupled-resonator systems [28–30]. These results may open up a pathway in photonics and offer prospects of smaller devices for the manipulation and transmission of light. Therefore, combining the EIT-like response with plasmonic structures would create the possibility of achieving ultracompact functional optical components for use in highly integrated optics [31].

In this paper, the spectral splitting behaviors based on EIT are numerically investigated in the compact plasmonic waveguide system consisting of a MIM waveguide coupled with stub and square ring resonators. The transmission properties of the system are simulated by the finite element method, and

Z. Chen · W. Wang · L. Cui · L. Yu · G. Duan · Y. Zhao · J. Xiao
State Key Laboratory of Information Photonics and Optical Communications, Beijing University of Posts and Telecommunications, Beijing 100876, China

Z. Chen · W. Wang · L. Cui · L. Yu (✉) · G. Duan · Y. Zhao · J. Xiao
School of Science, Beijing University of Posts and Telecommunications, Beijing 100876, China
e-mail: bupt.yuli@gmail.com

it is found that transparency window can be tuned by changing the geometrical parameters of the structure and the material filled in the resonators, and the spectrum can be effectively split by adding another stub or (and) square ring resonator. The physical mechanism is analyzed in detail. The proposed compact plasmonic structure may pave a new way for the design of multi-EIT-like splitter.

Structures and Simulations

The proposed plasmonic waveguide structure is schematically shown in Fig. 1a, which is composed of a MIM structure with a stub and a square ring resonator. This system is a two-dimensional model, and the white and blue parts denote air (ε_{d}=1.0) and Ag (ε_{m}), respectively. The width of the MIM waveguide, stub resonator, and the square ring are *w*, and *g* denotes the coupling distance between the stub and the square ring resonator. The length of the stub and square ring are *d* and *L*, respectively. The transmittance of SPPs is defined as the quotient between the SPP power flows (obtained by integrating the Poynting vector over the channel cross section) of the observing port with structures (stub and square ring resonator) and without structures.

In order to investigate the coupling effects, the transmission spectra of the proposed structure are numerically calculated using the finite element method (FEM) of COMSOL Multiphysics. Since the width of the bus waveguide is much smaller than the wavelength of the incident light, only a single propagation mode TM_0 can exist in the structure. In the simulations, the parameters g=10 nm and w=50 nm are fixed throughout the paper. The permittivity of Ag is characterized by the Drude model: $\varepsilon_{\mathrm{m}}=\varepsilon_{\infty}-\omega_p^2\,/\,(\omega^2+i\omega\gamma)$ with ε_{∞}=3.7, ω_{p}=9.1 eV, and γ=0.018 eV [28, 32]. Figure 1b shows the transmission spectra without and with a square ring resonator. It is found that the transmission spectrum exhibits a resonant dip at λ=1234 nm (d=200 nm), when the square ring resonator is removed, which is consistent with the results in [9, 33]. When the stub resonator is coupled with the square ring resonator, a narrow transmission peak is formed in the broad stop-band of the stub resonator. This is a typical EIT-like spectral response [22, 28], which is derived from a special coherent effect: the coherent interference between the two optical pathways, namely, the direct excitation of resonant mode in the stub by the incident wave and the excitation by coupling with the square ring resonator [30]. In other words, the broad resonant mode of the stub resonator is split into two resonant modes, one of them is blue shifted while the other is red shifted, which can be clearly seen in the transmission spectra in Fig. 1b. Figure 1c, d shows the field distributions of $|H_z|$ at the EIT-like transparency peak of 1234 nm without and with the square ring resonator. It can be seen from Fig. 1c that the incident wave is reflected in the single stub resonator. However, the electromagnetic field in the stub resonator is very weak, while there exist strongly enhanced fields in the square ring resonator due to the destructive interference between the two excitation pathways, as shown in Fig. 1d.

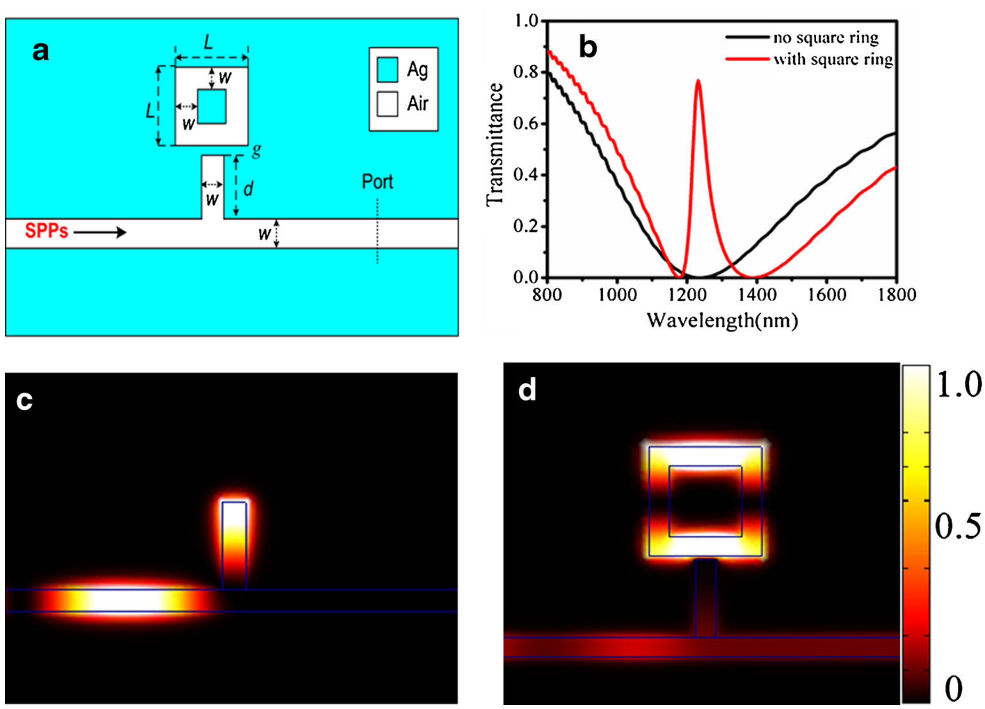

Fig. 1 **a** Schematic configuration and geometric parameters of the plasmonic waveguide system. **b** Transmission spectra without (*black curve*) and with (*red curve*) the square ring resonator. The parameters are set as d=200 nm and L=280 nm. **c**, **d** The $|H_z|$ field distributions without and with the square ring resonator at the resonance wavelength λ= 1234 nm

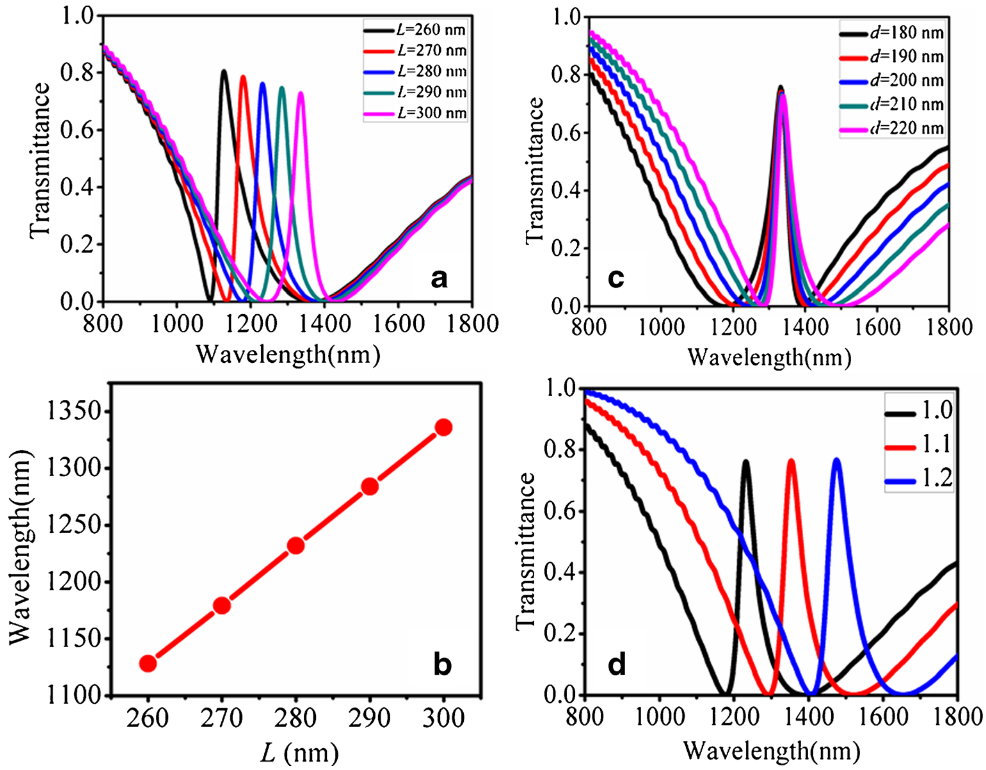

Fig. 2 **a** Transmission spectra for different length of the square ring resonator L with d=200 nm. **b** Resonance peak wavelength of the structure versus the length of the square ring resonators. **c** Transmission spectra for different length of the stub resonator d with L=300 nm. **d** Transmission spectra for different refractive index with d=200 nm and L=280 nm

Transmission Properties of the Proposed Structure with Different Parameters

As we know, the transmission characteristics of the plasmonics waveguide system can be affected by the structure parameters. First, we calculated the transmission spectra for different length of the square ring resonator L when d=200 nm and as shown in Fig. 2a. It is obvious that the resonance peak wavelength has a red shift with the increasing length L. Figure 2b shows the relationship between the resonance peak wavelength and the length L; it is found that the resonance peak wavelength has a linear relationship with the length L. Successively, we investigate the influence of the length of the stub resonator d on the resonance wavelength when L=300 nm and as shown in Fig. 2c. It is clearly that the resonance wavelength almost unchanged with d increasing or a fixed L. Furthermore, we investigate the influence of the material embedded in the resonators on the resonance peak wavelength. The parameters of

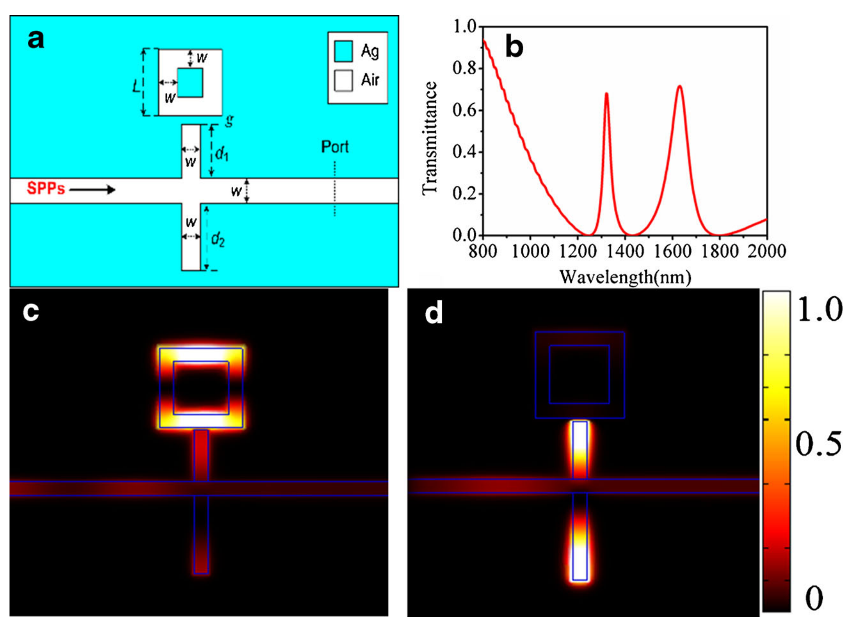

Fig. 3 **a** Schematic configuration and geometric parameters of the two stub resonators and a square ring resonator. **b** Transmission spectrum of the two stub resonators and a square ring resonator system. The parameters are set as d_1=200 nm, d_2=300 nm, and L=300 nm. The $|H_z|$ field distributions for the system at the resonance wavelengths **c** λ=1323 nm and **d** λ=1631 nm

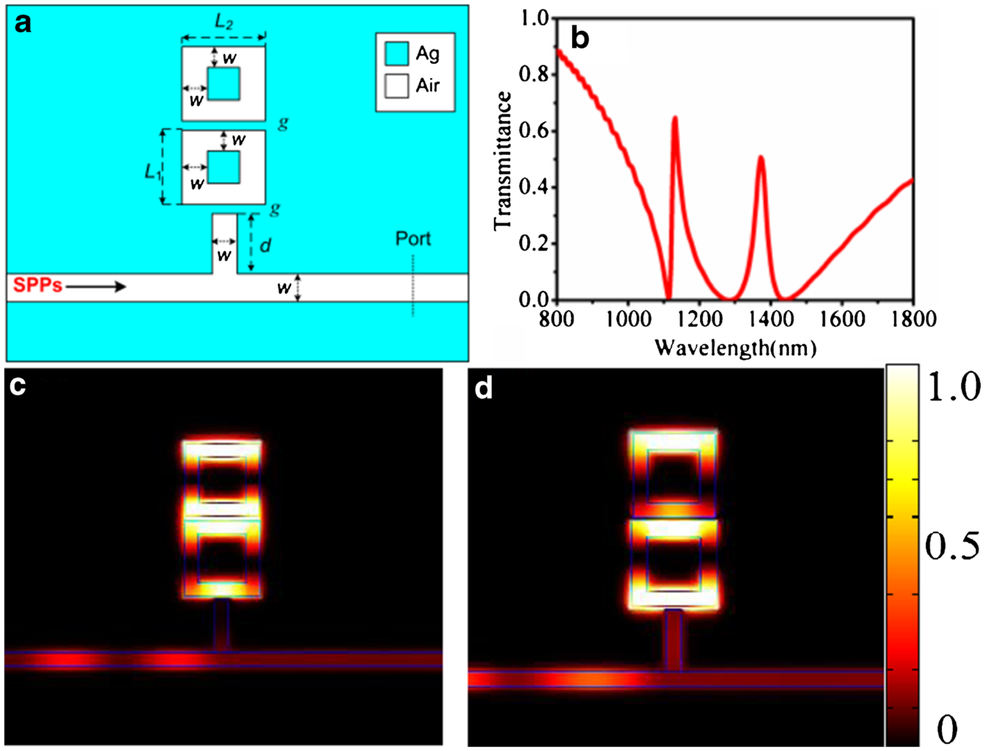

Fig. 4 **a** Schematic configuration and geometric parameters of a stub resonator and two square ring resonators. **b** Transmission spectrum of the system with a stub resonator and two square ring resonators. The parameters are set as L_1=300 nm, L_2= 280 nm, and d=200 nm. The $|H_z|$ field distributions for the system at the resonance wavelengths of **c** λ=1131 nm and **d** λ=1374 nm

the structure are set to be d=200 nm and L=280 nm. By changing the refractive index, the center wavelength exhibits a red shift as shown in Fig. 2d. The above conclusion can be explained by the standing wave theory in Ref. [16]. Even though the structure considered here is different from that in Ref. [16], both structures have similar mechanisms. Therefore, according to the results and analysis, one can easily manipulate the resonance wavelength by modifying the length of the square ring resonator L or fitting the material with appropriate refractive index in the resonators. Besides, the proposed structure can be served as a high sensitivity nanosensor with the sensitivity of 1230 nm/RIU (per unit variations of the refractive index) [4].

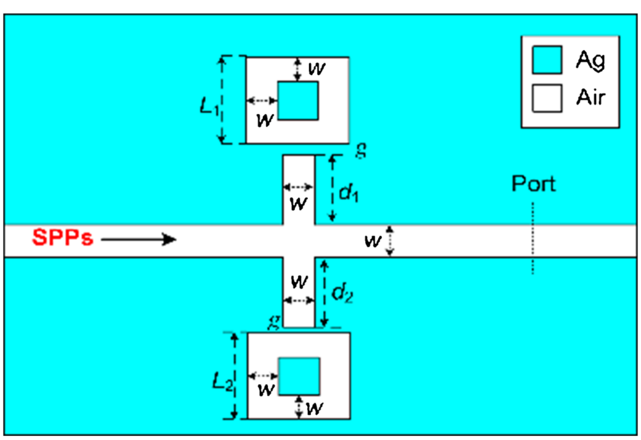

Fig. 5 Schematic configuration and geometric parameters of the plasmonic waveguide system with two stub resonators and two square ring resonators

Double EIT Induced by Adding a Stub or a Square Ring Resonator

The proposed EIT structure in Fig. 1a is flexible and can be easily extended to a double EIT system by adding another stub resonator, as shown in Fig. 3a. By carefully adjusting the parameters of the structure, two transmission peaks emerge, revealing two EIT-like optical response, as shown in Fig. 3b. In order to reveal the causes of these two peaks, the corresponding field distributions of $|H_z|$ at these two transmission peaks are displayed in Fig. 3c, d. At λ=1323 nm or the high energy EIT peak, it is easy to know that Figs. 3c and 1d have the same field distribution; therefore, they have the similar propagation behavior of SPPs in the upper stub and the square ring resonator, and it can be explained by the above analysis. However, the behavior of SPPs for the low energy EIT peak at λ=1631 nm may be different. We know that a stub resonator can act as a high reflector [29]. Thus, the SPPs reflected back and forth between the upper and lower stub resonators, constructing a Fabry–Perot (FP) resonator [27]. From Fig. 3d, we find that there exist strong field distributions between the two stub resonators; this means that the resonant enhancement occurs in the FP resonator, resulting in the transmission peaks.

Double EIT Induced by Adding a Square Ring Resonator

Besides, we can also achieve the double EIT-like transmission by adding another square ring resonator, as shown in Fig. 4a. The coupling distance between the two square ring

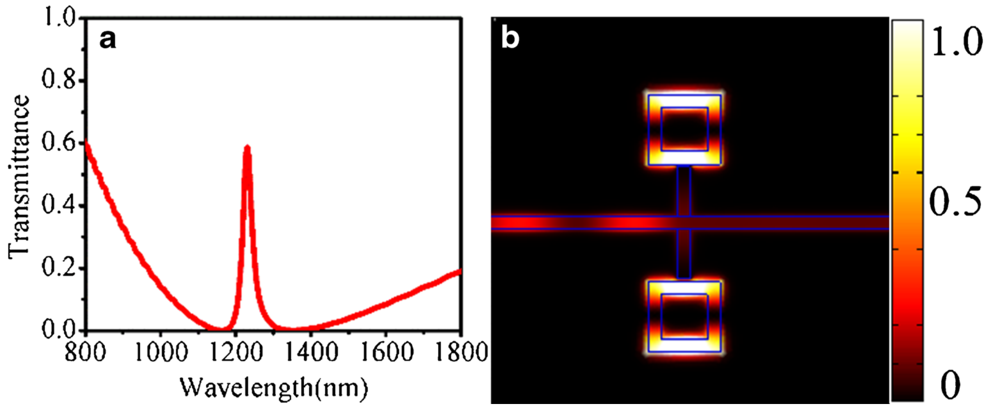

Fig. 6 **a** Transmission spectrum of the system with two stub resonators and two square ring resonators. The parameters are set as $d_1=d_2=200$ nm, and $L_1=L_2=280$ nm. **b** The $|H_z|$ field distributions for the system at the resonance wavelength $\lambda=1234$ nm

resonators is also denoted as g ($g=10$ nm). The FEM is used to calculate the transmission properties of the proposed structure, as shown in Fig. 4b. Obviously, two EIT peaks emerge in the wide transmission spectrum. The corresponding field distributions ($|H_z|$) at these two EIT peaks are displayed in Fig. 4c, d. This phenomenon is similar to the mode splitting according to the plasmon hybridization theory, which is used in the coupled metal nanoparticle systems [34]. From Fig. 3c, d, we can see that the MIM stub resonates weakly while the two square ring resonators resonate strongly, which is similar to the single EIT system shown in Fig. 1d. The difference between the two EIT peaks is that the phase of $|H_z|$ in the adjacent of the two square ring resonators are inphase and antiphase for the high energy EIT peak and low energy EIT peak, respectively. According to the above results, the resonance spectra are split because of the phase-coupled effects.

Transmission Properties of the System with two Stub and Square Ring Resonators

According to the above characteristics of the plasmonic system based on stub and square ring resonator (s), the properties of the structure, which consists of one stub coupled with a square ring resonator on each side of the MIM waveguide, is proposed and investigated. As shown in Fig. 5, the definition of the parameters are the same in Fig. 1a. Firstly, we study the transmission characteristics of the symmetric case: $d_1=d_2=200$ nm, $L_1=L_2=280$ nm. Figure 6a shows the transmission spectrum of the symmetric case, and the corresponding field distribution of $|H_z|$ is shown in Fig. 6b. The resonance feature in the plasmonic waveguide can be analyzed as discussed above in "Structures and Simulations." Furthermore, it is clearly that the wideband of the transparency window is much narrower

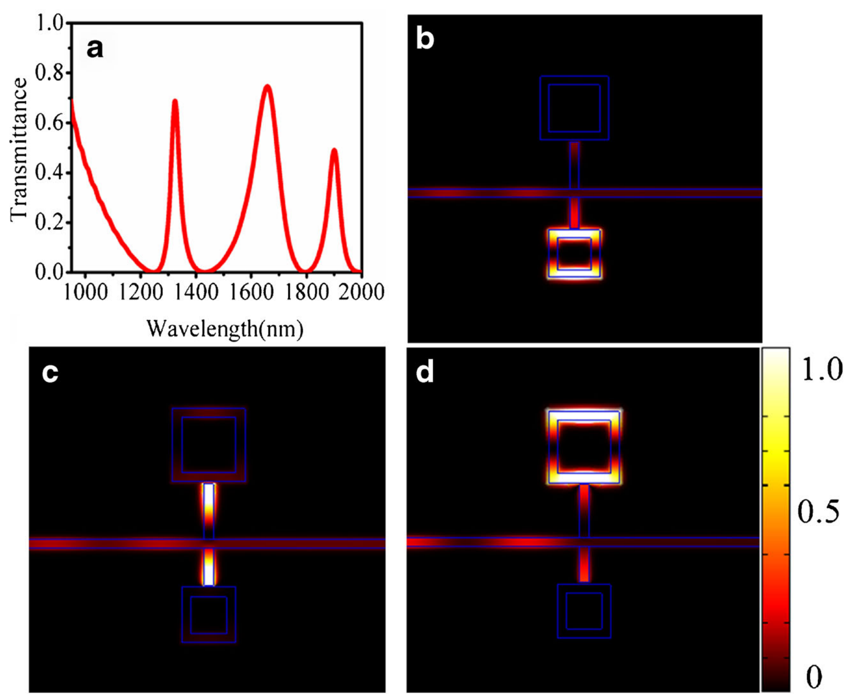

Fig. 7 **a** Transmission spectrum of the system with two stub resonators and two square ring resonators. The parameters are set as $d_1=200$ nm, $L_1=300$ nm, $d_2=300$ nm, and $L_2=400$ nm. The $|H_z|$ field distributions for the system at the resonance wavelengths **b** $\lambda=1323$ nm, **c** $\lambda=1659$ nm, and **d** $\lambda=1902$ nm

with the transmittance a little lower compared to the spectrum of the single structure in Fig. 1b.

Next, we discuss the properties of the proposed structure for the general case: d_1=200 nm, L_1=300 nm, d_2=300 nm, and L_2=400 nm. It is obvious that three transmission peaks occur in the broadband transmission spectrum, revealing three-EIT-like optical response as shown in Fig. 7a. The corresponding field distributions of $|H_z|$ at these transmission peaks are displayed in Fig. 7b–d. These strong field distributions also reveal the generation mechanism of their own as discussed above. The multiresonator-coupled system with multi-EIT-like optical responses may have complex functional applications, such as channel selection, channel add–drop, multichannel switches, and wavelength-division multiplexing.

Conclusions

In this paper, we have designed several kinds of spectral splitters based on the EIT-like transmission in a nanoscale plasmonic waveguide resonator system. The transmission properties of the structure have been investigated by the FEM simulations. The transparency window can be easily tuned by changing the geometrical parameters of the structure and the material filled in the resonators. By adding another stub or square ring resonator, multi-EIT-like peaks appear in the broadband transmission spectrum due to the emerging of the new resonator or the phase-coupled effect. The proposed plasmonic structures may have potential applications for nanoscale optical switching, nanosensor, and slow-light devices in highly integrated optical circuits.

Acknowledgments This work was supported by the National Natural Science Foundation of China under Grant No. 11374041, National Basic Research Program of China under Grant No. 2010CB923202 and Fund of State Key Laboratory of Information Photonics and Optical Communications (Beijing University of Posts and Telecommunications), People's Republic of China.

References

1. Barnes WL, Dereux A, Ebbesen TW (2003) Surface plasmon subwavelength optics. Nature 424(6950):824–830
2. Lu H, Liu XM, Wang LR, Gong YK, Mao D (2011) Ultrafast all-optical switching in nanoplasmonic waveguide with Kerr nonlinear resonator. Opt Express 19(4):2910–2915
3. Xiao SS, Liu L, Qiu M (2006) Resonator channel drop filters in a plasmon-polaritons metal. Opt Express 14(7):2932–2937
4. Chen JJ, Li Z, Yue S, Xiao JH, Gong QH (2012) Plasmon-induced transparency in asymmetric T-shape single slit. Nano Lett 12(5): 2494–2498
5. Lu H, Liu XM, Mao D, Wang GX (2012) Plasmonic nanosensor based on Fano resonance in waveguide-coupled resonators. Opt Lett 37(18):3780–3782
6. Xu T, Wu YK, Luo XG, Guo LJ (2010) Plasmonic nanoresonators for high-resolution colour filtering and spectral imaging. Nature Commun 1:59
7. Veronis G, Fan SH (2005) Bends and splitters in metal-dielectric-metal subwavelength plasmonic waveguides. Appl Phys Lett 87: 131102
8. Economou EN (1969) Surface plasmons in thin films. Phys Rev 182: 539
9. Lin XS, Huang XG (2008) Tooth-shaped plasmonic waveguide filters with nanometeric sizes. Opt Lett 33(23):2874–2876
10. Hosseini A, Massoud Y (2007) Nanoscale surface plasmon based resonator using rectangular geometry. Appl Phys Lett 90:181102
11. Zhang Q, Huang XG, Lin XS, Tao J, Jin XP (2009) A subwavelength coupler-type MIM optical filter. Opt Express 17(9):7549–7554
12. Tao J, Huang XG, Lin XS, Zhang Q, Jin XP (2009) A narrow-band subwavelength plasmonic waveguide filter with asymmetrical multiple teeth-shaped structure. Opt Express 17(16):13989–13994
13. Chen JJ, Li Z, Lei M, Fu XL, Xiao JH, Gong QH (2012) Plasmonic Y-splitters of high wavelength resolution based on strongly coupled-resonator effects. Plasmonics 7(3):441–445
14. Guo YH, Yan LS, Pan W, Luo B, Wen KH, Guo Z, Li HY, Luo XG (2011) A plasmonic splitter based on slot cavity. Opt Express 19(15): 13831–13838
15. Chen JJ, Li Z, Zou YJ, Deng ZL, Xiao JH, Gong QH (2013) Coupled-resonator-induced fano resonances for plasmonic sensing with ultra-high figure of merits. Plasmonics 8:1627–1632
16. Zhou ZP, Hu FF, Yi HX (2011) Wavelength demultiplexing structure based on arrayed plasmonic slot cavities. Opt Lett 36(8):1500–1502
17. Wang GX, Lu H, Liu XM, Mao D, Duan LN (2011) Tunable multi-channel wavelength demultiplexer based on MIM plasmonic nanodisk resonators at telecommunication regime. Opt Express 19(4): 3513–3518
18. Noual A, Akjouj A, Pennec Y, Gillet J, Djafari-Rouhani B (2009) Modeling of two-dimensional nanoscale Y-bent plasmonic waveguides with cavities for demultiplexing of the telecommunication wavelengths. New J Phys 11(10):103020
19. Lu H, Liu XM, Gong YK, Mao D, Wang LR (2011) Enhancement of transmission efficiency of nanoplasmonic wavelength demultiplexer based on channel drop filters and reflection nanocavities. Opt Express 19(14):12885–12890
20. Boller KJ, Imamoglu A, Harris SE (1991) Observation of electromagnetically induced transparency. Phys Rev Lett 66(20):2593
21. Fleischhauer M, Imamoglu A, Marangos JP (2005) Electromagnetically induced transparency: optics in coherent media. Rev Mod Phys 77:633–673
22. Xu Q, Sandhu S, Povinelli ML, Shakya J, Fan S, Lipson M (2006) Experimental realization of an on-chip all-optical analogue to electromagnetically induced transparency. Phys Rev Lett 96: 123901
23. Naweed A, Farca G, Shopova SI, Rosenberger AT (2005) Induced transparency and absorption in coupled whispering-gallery microresonators. Phys Rev A 71:043804
24. Liu HC, Amnon Y (2009) Grating induced transparency (GIT) and the dark mode in optical waveguides. Opt Express 17(14):11710–11718
25. Yang X, Yu M, Kwong DL, Wong CW (2009) All-optical analog to electromagnetically induced transparency in multiple coupled photonic crystal cavities. Phys Rev Lett 102:173902
26. Zhou JH, Mu D, Yang JH, Han WB, Di X (2011) Coupled-resonator-induced transparency in photonic crystal waveguide resonator systems. Opt Express 19(5):4856–4861
27. Kekatpure RD, Barnard ES, Cai WS, Brongersma ML (2010) Phase-coupled plasmon-induced transparency. Phys Rev Lett 104:243902
28. Lu H, Liu X, Mao D, Gong Y, Wang G (2011) Induced transparency in nanoscale plasmonic resonator systems. Opt Lett 36(16):3233–3235

29. Chen JJ, Wang C, Zhang R, Xiao JH (2013) Multiple plasmon-induced transparencies in coupled-resonator systems. Opt Lett 37(24):5133–5135
30. Lu H, Liu XM, Wang GX, Mao D (2012) Tunable high-channel-count bandpass plasmonic filters based on an analogue of electromagnetically induced transparency. Nanotech 23:444003
31. Liu N, Langguth L, Weiss T, Kastel J, Fleisch M, Pfau T, Giedden H (2009) Plasmonic analogue of electromagnetically induced transparency at the Drude damping limit. Nat Mater 8:758–762
32. Han Z, Forsberg E, He S (2007) Surface plasmon Bragg gratings formed in metal-insulator-metal waveguides. IEEE Photon Technol Lett 19:91–93
33. Matsuzaki Y, Okamoto T, Haraguchi M, Fukui M, Nakagaki M (2008) Characteristics of gap plasmon waveguide with stub structures. Express 16(21):16314–16325
34. Nordlander P, Oubre C, Prodan E, Li K, Stockman MI (2004) Plasmon hybridization in nanoparticle dimers. Nano Lett 4(5):899–903